Dual-Mode EPR Study of Mn(III) Salen and the Mn(III) Salen-Catalyzed Epoxidation of *cis*-β-Methylstyrene

Kristy A. Campbell,*,† Matthew R. Lashley, Justin K. Wyatt, Michael H. Nantz, and R. David Britt*

Contribution from the Department of Chemistry, University of California, Davis, California 95616

Received July 25, 2000. Revised Manuscript Received January 30, 2001

Abstract: Dual-mode electron paramagnetic resonance (EPR), in which an oscillating magnetic field is alternately applied parallel or perpendicular to the static magnetic field, is a valuable technique for studying both half-integer and integer electron spin systems and is particularly useful for studying transition metals involved in redox chemistry. We have applied this technique to the characterization of the Mn(III) salen (salen = *N*,*N*′-ethylene bis(salicylideneaminato)) complex [(*R*,*R*)-(−)-*N*,*N*′-bis(3,5-di-*tert*-butylsalicylidene)-1,2-cyclohexanediaminomanganese(III)], with an $S = 2$ integer electron spin system. Furthermore, we have used dual-mode EPR to study the Mn salen complex during the Mn(III) salen-catalyzed epoxidation of cis-β-methylstyrene. Our study shows that the additives *N*-methylmorpholine *N*-oxide (NMO) and 4-phenylpyridine-*N*-oxide (4-PPNO), which are used to improve epoxidation yields and enantioselection, bind to the Mn(III) center prior to the epoxidation reaction, as evidenced by the alteration of the Mn(III) parallel mode EPR signal. With these additives as ligands, the axial zero-field splitting values and ^{55}Mn hyperfine splitting of the parallel mode signal are indicative of an axially elongated octahedral geometry about the Mn(III) center. Since the dual-mode EPR technique allows the observation of both integer and half-integer electron spin systems, Mn oxidation states of II, III, IV, and potentially V can be observed in the same sample as well as any radical intermediates or Mn(III,IV) dinuclear clusters formed during the Mn(III) salen-catalyzed epoxidation reaction. Indeed, our study revealed the formation of a Mn(III,IV) dinuclear cluster in direct correlation with expoxide formation. In addition to showing the possible reaction intermediates, dual-mode EPR offers insight into the mechanism of catalyst degradation and formation of unwanted byproducts. The dual-mode technique may therefore prove valuable for elucidating the mechanism of Mn(III) salen catalyzed reactions and ultimately for designing optimum catalytic conditions (solvents, oxidants, and additives such as NMO or 4-PPNO).

Mn(III) salen complexes are excellent catalysts for the highly enantioselective asymmetric epoxidation of olefins.[1] However, the exact mechanism of the formation of epoxides in this catalytic reaction is unknown. For conjugated olefins, such as *cis*-β-methylstyrene, it is believed that the Mn(III) salen complex is initially oxidized to a Mn(V)═O species,[1−4] which subsequently participates in oxygen atom transfer to the olefin via either direct substrate attack at the oxo ligand in a stepwise radical intermediate process[5] or via substrate attack at both the Mn center and the oxo ligand (via an Mn(IV) oxametallic intermediate).[6] Other models for Mn(III) salen-catalyzed epoxidation reactions propose an equilibrium between a Mn(V)═O species and a μ-oxomanganese(IV) dimer, with the rate-limiting step determined by the rate of disproportionation of the μ-oxomanganese(IV) dimer to the active Mn(V)═O species responsible for oxygen atom transfer to the olefin.[2] Models proposing a μ-oxomanganese(IV) dimer also have been invoked for closely related epoxidation reactions catalyzed by Mn(III) porphyrin systems.[7] In addition, a mechanism has been proposed for the corresponding Mn(III) porphyrin-catalyzed epoxidation of olefins in which there are two reaction pathways competing for the olefin: one involving a Mn(V)═O species and the other involving a Mn(IV)═O species.[8] The Mn(IV)═O species is assigned to a nonstereoretentive pathway, whereas the Mn(V)═O pathway is credited for producing epoxides with retention of configuration. This competing reaction pathway mechanism may also be at work in the Mn(III) salen-catalyzed epoxidation reactions.

Interestingly, almost all models for the Mn(III) salen-catalyzed epoxidation of *cis*-β-methylstyrene agree that a Mn(V)═O species is responsible for the high enantioselectivity of the epoxidation reaction even though there has been no absolute direct evidence for the existence of this species. In one

* To whom correspondence should be addressed.

† Current address: Micron Technology, Inc., 8000 S. Federal Way, Boise, ID 83707.

(1) (a) Katsuki, T. *J. Mol. Catal. A* **1996**, *113*, 87−107. (b) Jacobsen, E. N. Asymmetric Catalytic Epoxidation of Unfunctionalized Olefins. In *Catalytic Asymmetric Synthesis*; Ojima, I., Ed.; VCH Publishers: New York, 1993; pp 159−202. (c) Stephenson, G. R. Asymmetric Oxidation. In *Advanced Asymmetric Synthesis*; Stephenson, G. R., Ed.; Chapman & Hall: New York, 1996; pp 367−391. (d) Jørgensen, K. A. *Chem. Rev.* **1989**, *89*, 431−458.

(2) Srinivasan, K.; Michaud, P.; Kochi, J. K. *J. Am. Chem. Soc.* **1986**, *108*, 2309−2320.

(3) Feichtinger, D.; Plattner, D. A. *Angew. Chem., Int. Ed. Engl.* **1997**, *36*, 1718−1719.

(4) Palucki, M.; Finney, N. S.; Pospisil, P. J.; Güler, M. L.; Ishida, T.; Jacobsen, E. N. *J. Am. Chem. Soc.* **1998**, *120*, 948−954.

(5) Finney, N. S.; Pospisil, P. J.; Chang, S.; Palucki, M.; Konsler, R. G.; Hansen, K. B.; Jacobsen, E. N. *Angew. Chem., Int. Ed. Engl.* **1997**, *36*, 1720−1723.

(6) Linde, C.; Arnold, M.; Norrby, P.-O.; Akermark, B. *Angew. Chem., Int. Ed. Engl.* **1997**, *36*, 1723−1725.

(7) Smegal, J. A.; Schardt, B. C.; Hill, C. L. *J. Am. Chem. Soc.* **1983**, *105*, 3510−3515.

(8) (a) Groves, J. T.; Stern, M. K. *J. Am. Chem. Soc.* **1987**, *109*, 3812−3814. (b) Groves, J. T.; Stern, M. K. *J. Am. Chem. Soc.* **1988**, *110*, 8628−8638.

10.1021/ja0027463 CCC: $20.00
Published on Web 05/26/2001

report, an electrospray tandem mass spectrometry study of the [Mn(III) salen($NCCH_3$)]$^+$-catalyzed epoxidation of cyclohexene, using iodosobenzene in acetonitrile as the oxidant, detected a [(salen)Mn(V)═O]$^+$ intermediate; however, whether the origin of this species is an actual intermediate of the epoxidation reaction or simply a fragmentation product from a μ-oxomanganese(IV) dimer (as assigned in the mass spectrum) is unknown.[3] Additional support for the existence of a Mn(V)═O species comes from analogy with similar Cr(III) salen-catalyzed epoxidation reactions which proceed via a Cr(V)═O complex.[9] A Cr(V)═O has been characterized from both Cr salen and Cr porphyrin complexes.[9−11] This lends support for analogies to be made between the Mn(III) salen complex and the Mn(III) porphyrin systems where an intermediate species, assigned to a Mn(V)═O species on the basis of its reactivity, was detected via stopped-flow UV−vis spectroscopy during oxidation of [Mn(III)TMPyP] (TMPyP = tetra(*N*-methylpyridyl)porphyrinatomanganese(III)).[12]

Additives to the Mn(III) salen reaction mixture, such as NMO and 4-PPNO, generally facilitate faster reaction rates, higher epoxide yields, and improved enantioselectivity.[5,13−16] This improvement has been attributed in part to the depression of Lewis acidity of the Mn ion upon coordination of the donor ligand.[1*a*] Exactly when the donor ligand binds to the Mn ion has not been previously determined; however, based on experimental results showing an increase in reaction rates upon addition of an *N*-oxide additive it has been suggested that the additive binds to the metal after the rate-limiting generation of the reactive Mn(V)═O intermediate.[5]

Until now, spectroscopic observation of the Mn(III) salen complex during the epoxidation reaction has been limited to UV−vis[2] and ^{1}H NMR[17] studies. These studies show spectral signatures that have been attributed to a Mn(IV), a Mn(IV)−O−Mn(IV) dimer, and a Mn(V) species. However, the lack of spectral resolution and absolute spectral assignment limit these spectroscopic techniques. We have thus applied dual-mode EPR to characterization of Mn(III) salen and to the in situ study of the epoxidation of *cis*-β-methylstyrene by Mn(III) salen. The dual-mode EPR technique encompasses both perpendicular and parallel polarization EPR. The technique of parallel polarization EPR is useful for observing EPR spectra from integer electron spin systems such as found in many transition metals (e.g., Mn(III)), whereas conventional perpendicular mode EPR allows observation of half integer spin systems (e.g., Mn(IV), mixed-valent ^{55}Mn clusters, organic radicals). We have previously used parallel polarization EPR to obtain hyperfine resolved spectra of integer spin Mn(III) complexes (d,[4] $S = 2$ systems),[18] erroneously believed to be EPR silent.[19*a*] Parallel polarization EPR studies of Mn(III) in the manganese superoxide dismutase enzyme[18*a*] and in Photosystem II[18b−d] coupled with our characterization of Mn(III) salen in this work show that parallel polarization EPR is a powerful tool for elucidation of zero-field splitting values and metal center geometry. Thus, the dual-mode EPR spectroscopic technique is ideally suited for observation of the Mn(III) salen catalysts since the Mn(III) salen catalyst can be spectroscopically monitored with EPR while also monitoring the generation of other paramagnetic species such as Mn(IV) complexes or radicals. The proposed Mn(V)═O intermediate is predicted to present either a diamagnetic ($S = 0$), triplet ($S = 1$), or quintet ($S = 2$) spin state during the epoxidation reaction course.[20,21] Both of the possible integer spin ($S = 1$ or 2) states would be observable with parallel mode X-band EPR if the Mn ion zero-field splitting parameters are in an appropriate range.

Materials and Methods

Mn(III) Salen EPR Sample Preparation. Mn(III)salen (Jacobsen's catalyst, Aldrich Chemical Co. [(*R*,*R*)-(−)-*N*,*N*-bis(3,5-di-*tert*-butylsalicylidene)-1,2-cyclohexanediaminomanganese(III) chloride]) EPR samples were prepared with either NMO or 4-PPNO, or without, in dry CH_2Cl_2. Samples were added to quartz EPR tubes (Wilmad Glass, SQ-707) to a final Mn salen concentration of 1 mM. NMO and 4-PPNO, when included, were added as 100 and 20 equiv of the Mn(III) salen concentration, respectively.

Reaction Procedures. Epoxidation reactions were performed using Mn(III) salen in CH_2Cl_2 with *cis*-β-methylstyrene (TCI). The oxidants used were *m*-chloroperoxybenzoic acid (*m*-CPBA) or NaOCl. NMO was added to the Mn(III) salen in CH_2Cl_2 for the reaction that employed *m*-CPBA as an oxidant. Reactions using NaOCl as the oxidant were performed with and without the additive 4-PPNO.

Three different methods of performing the epoxidation reaction were used. In Method 1, the reaction mixtures of Mn(III) salen, styrene, an additive, and oxidant were prepared in batch according to the procedures of Jacobsen.[13,22−24] After the commencement of the reaction, aliquots were removed at specific times and immediately loaded into EPR tubes at the temperature of the reaction bath, capped with rubber septa, then immediately transferred to liquid nitrogen (77 K) to stop the reaction.

In Method 2, reactions were performed in EPR tubes rather than in batch as in Method 1. In this case, a solution of the Mn(III) salen-NMO-styrene in CH_2Cl_2 and a separate solution of *m*-CPBA in CH_2Cl_2 were prepared. A cold (195 K; kept in a dry ice/methanol bath) EPR tube was loaded with the Mn(III) salen-NMO-styrene mixture. The tube was cooled to 175 K (submerged in a methanol/liquid nitrogen bath) to freeze the Mn(III) salen-styrene mixture. The *m*-CPBA solution was added to the top surface of the frozen Mn(III) salen-styrene mixture in the EPR tube and immediately quenched in liquid nitrogen (77 K) without any mixing into the Mn(III) salen layer. Method 2 was used to observe the reaction progress as the sample was successively warmed slightly above 175 K and the *m*-CPBA layer was allowed to react with the Mn(III) salen-styrene layer for controlled time periods. Plastic syringes and tubing were used to load all EPR tubes when *m*-CPBA

(9) Samsel, E. G.; Srinivasan, K.; Kochi, J. K. *J. Am. Chem. Soc.* **1985**, *107*, 7606−7617.
(10) Siddall, T. L.; Miyaura, N.; Huffman, J. C.; Kochi, J. K. *J. Chem. Soc., Chem. Commun.* **1983**, 1185−1186.
(11) Groves, J. T.; Kruper, W. J., Jr. *J. Am. Chem. Soc.* **1979**, *101*, 7613−7615.
(12) Groves, J. T.; Lee, J.; Marla, S. S. *J. Am. Chem. Soc.* **1997**, *119*, 6269−6273.
(13) Palucki, M.; Pospisil, P. J.; Zhang, W.; Jacobsen, E. N. *J. Am. Chem. Soc.* **1994**, *116*, 9333−9334.
(14) Irie, R.; Ito, Y.; Katsuki, T. *SYNLETT* **1991**, 265−266.
(15) Miura, K.; Katsuki, T. *SYNLETT* **1999**, 783−785.
(16) Pietikäinen, P. *Tetrahedron Lett.* **1994**, *35*, 941−944.
(17) Bryliakov, K. P.; Babushkin, D. E.; Talsi, E. P. *Mendeleev Commun.* **2000**, 1−42.
(18) (a) Campbell, K. A.; Yikilmaz, E.; Grant, C. V.; Gregor, W.; Miller, A.-F.; Britt, R. D. *J. Am. Chem. Soc.* **1999**, *121*, 4714−4715. (b) Campbell, K. A.; Force, D. A.; Nixon, P. J.; Dole, F.; Diner, B. A.; Britt, R. D. *J. Am. Chem. Soc.* **2000**, *122*, 3754−3761. (c) Britt, R. D.; Peloquin, J. M.; Campbell, K. A. *Annu. Rev. Biophys. Biomol. Struct.* **2000**, *29*, 463−495. (d) Campbell, K. A. CW and Pulsed EPR of Photosystem II and Mn-Containing Complexes, Ph.D. Disstertation, University of CA, Davis, 1999.
(19) (a) Indeed, even recent work on EPR characterization of the Mn(IV) species generated during the Mn(III) salen epoxidation reaction[19b] states that Mn(III) is EPR inactive. (b) Adam, W.; Mock-Knoblauch; Saha-Møller, C. R.; Herderich, M. *J. Am. Chem. Soc.* **2000**, *122*, 9685−9691.
(20) Strassner, T.; Houk, K. N. *Org Lett.* **1999**, *1*, 419−421.
(21) Linde, C.; Åkermark, B.; Norrby, P.-O.; Svensson, M. *J. Am. Chem. Soc.* **1999**, *121*, 5083−5084.
(22) Lee, N. H.; Muci, A. R.; Jacobsen, E. N. *Tetrahedron Lett.* **1991**, *32*, 5055−5058.
(23) Jacobsen, E. N.; Zhang, W.; Muci, A. R.; Ecker, J. R.; Deng, L. *J. Am. Chem. Soc.* **1991**, *113*, 7063−7064.
(24) Palucki, M.; McCormick, G. J.; Jacobsen, E. N. *Tetrahedron Lett.* **1995**, *36*, 5457−5460.

Table 1. Summary of Reaction Procedures

reaction	styrene/additive	oxidant
Method 1: batch reactions		
A	*cis*-β-methylstyrene	NaOCl
B	*cis*-β-methylstyrene/4-PPNO	NaOCl
C	*cis*-β-methylstyrene/NMO	*m*-CPBA
D	None	NaOCl
Method 2: EPR tube reactions		
A	*cis*-β-methylstyrene/NMO	*m*-CPBA
Method 3: freeze-quench reactions		
A	*cis*-β-methylstyrene/NMO	*m*-CPBA

was used as an oxidant since it was found that the *m*-CPBA reacts with stainless steel needles and releases copper into the reaction mixtures (as evidenced by the presence of a Cu^{2+} EPR signal).

In Method 3, the reaction was performed using a freeze-quench technique. In this case, a solution of the Mn(III) salen-NMO-styrene in CH_2Cl_2 and a separate solution of *m*-CPBA in CH_2Cl_2 were prepared. The two separate solutions were each loaded into a syringe. Freeze-quench experiments were performed using an Update Instruments freeze-quench system with the Model 715 Syringe RAM controller, to capture the reaction products on the millisecond time scale. The samples were forced from the syringes into a mixing chamber where the solutions were mixed and immediately ejected through a single line of tubing whose length determined the reaction time. Reaction times varied from 50 to 500 ms. The syringe tips and tubing were composed of PEEK material to avoid degredation from the *m*-CPBA solution and CH_2Cl_2. All O-rings that were in contact with any CH_2Cl_2 were Viton. The reaction conditions for each of the methods are outlined below and summarized in Table 1.

Method 1: Reaction A. Following the procedure of Zhang and Jacobsen,[25] *cis*-β-methylstyrene (0.260 mL, 2.0 mmol) was added to a solution of Mn(III) salen (13 mg, 0.02 mmol) in dry CH_2Cl_2 (2 mL) at room temperature. NaOCl solution (pH 11.3, 9.1 mL, 5.0 mmol) was added to the Mn salen solution. The biphasic mixture was stirred at room temperature. At selected time points (including one prior to addition of the bleach solution) approximately 150 μL aliquots were withdrawn from the mixture and transferred to EPR tubes and subsequently frozen at 77 K. After being stirred for 3 h, the reaction mixture was quenched.[25] In a simultaneous experiment, in which no aliquots were removed for EPR analysis, this procedure yielded 54% of *cis*-β-methylstyrene oxide.

Method 1: Reaction B. A reaction mixture with 4-PPNO was prepared as in Zhang and Jacobsen[25] with the number of equivalents of 4-PPNO added as in Finney et al.[5] *cis*-β-Methylstyrene (0.130 mL, 1.0 mmol) was added to a solution of Mn(III) salen (6.3 mg, 0.01 mmol) and 4-PPNO (34 mg, 0.2 mmol) in dry CH_2Cl_2 (1.0 mL), followed by the addition of NaOCl solution (pH 11.3, 4.5 mL, 2.5 mmol). The reaction mixture was stirred at room temperature and EPR aliquots were removed as in Method 1, reaction A. In a parallel experiment, in which no aliquots were removed for EPR analysis, this procedure yielded 84% of *cis*-β-methylstyrene oxide.

Method 1: Reaction C. NMO (1.93 mmol) and *cis*-β-methylstyrene (50 μL, 0.385 mmol) were added at room temperature to a solution of Mn(III) salen (0.0193 mmol) in 2.4 mL of dry CH_2Cl_2. This solution was cooled to 195 K and a solution of *m*-CPBA (0.770 mmol) in CH_2Cl_2 (1.4 mL) was added. The reaction was stirred at 195 K during the entire reaction process. Aliquots for EPR were removed prior to the addition of *m*-CPBA and at succesive time intervals after addition of *m*-CPBA.

Method 1: Reaction D. A control reaction was run exactly as in Method 1, reaction A except that no styrene was added to the reaction mixture.

Method 2: Reaction A. A solution of Mn(III) salen-*cis*-β-methylstyrene-NMO was prepared as in Method 1, reaction C. An aliquot (110 μL) of this solution was added to an EPR tube at 195 K and cooled to 175 K (thus freezing the sample) followed by addition of an *m*-CPBA solution (65 μL, prepared as in Method 1, reaction C) to the top surface of the frozen Mn(III) salen solution. The EPR tube was then frozen in liquid nitrogen (77 K).

(25) Zhang, W.; Jacobsen, E. N. *J. Org. Chem.* **1991**, *56*, 2296−2298.

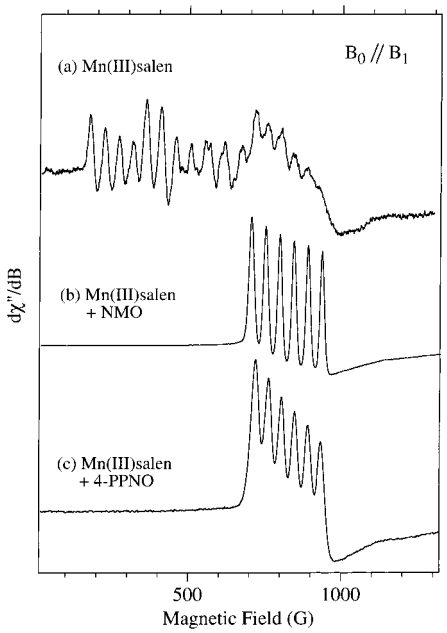

Figure 1. Parallel polarization CW-EPR of Mn(III) salen: (a) no additives; (b) with NMO; and (c) with 4-PPNO. Experimental conditions: microwave frequency, 9.393 GHz; microwave power, 1 mW; modulation amplitude, 10 G; modulation frequency, 100 kHz; time constant, 20.48 ms; conversion time, 40.96 ms; temperature 4.4 K, except (a) which is 2.7 K.

Method 3: Reaction A. Two solutions of Mn(III) salen-*cis*-β-methylstyrene-NMO (Flask A) and of MCPBA in CH_2Cl_2 (Flask B) were prepared as follows. Flask A contained 0.8 mmol of *cis*-β-methylstyrene, 4.0 mmol of NMO, and 0.04 mmol of Mn(III) salen in 5.0 mL of CH_2Cl_2. Flask B contained 0.32 M MCPBA in CH_2Cl_2. One-milliliter aliquots of the Mn(III) salen-styrene-NMO and *m*-CPBA solutions were loaded into separate syringes of the freeze-quench system. Seventy-five microliters was ejected from each syringe simultaneously into a mixing chamber and subsequently into an EPR tube. The overall reactant stoichiometry was thus similar to that in Method 1, reaction C. After each trial, the mixing chamber was cleaned to avoid contamination with "aged" reaction product in the next trial.

NMR Spectroscopy. NMR spectra were recorded on a GE QE-300 (300 MHz) spectrometer for the samples from Method 1, reactions A and B. In each case, the NMR spectra confirmed formation of *cis*-β-methylstyrene oxide: ^{1}H NMR, $CDCl_3$ δ 7.38−7.28 (m, 5H), 4.09 (d, J = 4.1 Hz, 1H), 3.77 (dq, J = 4.4 Hz, J = 5.4 Hz, 1H), 1.12 (d, J = 5.4 Hz, 3H).

EPR Spectroscopy. Continuous-wave EPR spectra were recorded on a Bruker ECS106 X-band CW-EPR system with a Bruker ER 4116DM dual mode cavity capable of both parallel (TE012) and perpendicular (TE102) mode polarizations of the applied magnetic field. Cryogenic temperatures were obtained with an Oxford ESR900 liquid helium cryostat. The temperature was controlled with an Oxford ITC503 temperature and gas flow controller. The microwave frequency was measured with a Hewlett-Packard X532B frequency meter equipped with a Hewlett-Packard X485B detector mount and detector.

EPR Spectral Simulation Methodology. Spectral simulations were performed for the Mn(III) salen EPR spectra as previously described.[18]

Results and Discussion

Characterization of Mn(III) Salen. Parallel and perpendicular mode CW-EPR spectra of the Mn(III) salen catalyst in CH_2Cl_2 with and without the additives NMO and 4-PPNO are shown in Figures 1 and 2, respectively. The parallel mode EPR spectrum of Mn(III) salen without an additive (Figure 1a) is complicated, consisting of many (>16) ^{55}Mn hyperfine lines.

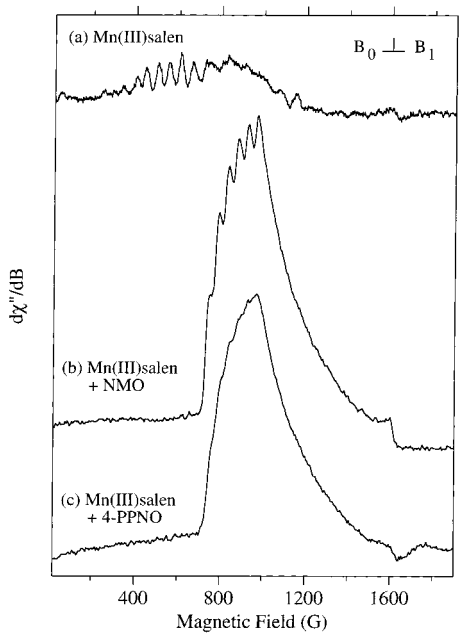

Figure 2. Perpendicular polarization CW-EPR of Mn(III) salen: (a) no additives; (b) with NMO; and (c) with 4-PPNO. Experimental conditions: microwave frequency, 9.667 GHz; microwave power, 1 mW; modulation amplitude, 10 G; modulation frequency, 100 kHz; time constant, 40.96 ms; conversion time, 81.92 ms; temperature 4.4 K, except (a) which is 2.7 K.

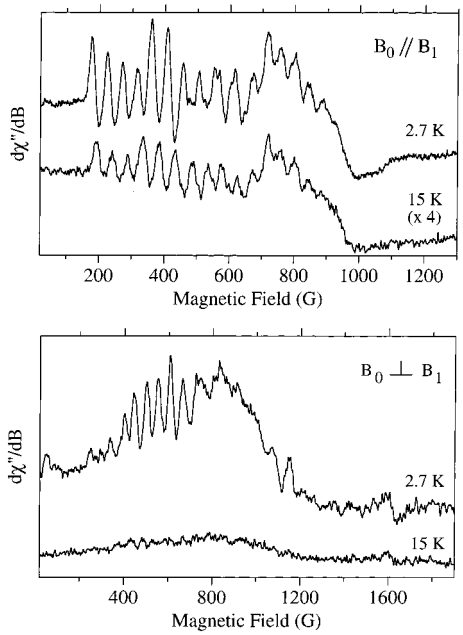

Figure 3. Parallel and perpendicular polarization CW-EPR of Mn(III) salen in CH_2Cl_2 without an additive at temperatures of 2.7 and 15 K. The parallel mode spectra (top graph) show at least 16 hyperfine lines. The lower field hyperfine lines at 15 K do not align with those at 2.7 K; however, the six highest field lines do align. The perpendicular mode (bottom graph) spectrum at 2.7 K shows hyperfine structure that is virtually gone at 15 K. Experimental conditions are the same as Figure 1 (parallel mode spectra) and Figure 2 (perpendicular mode spectra).

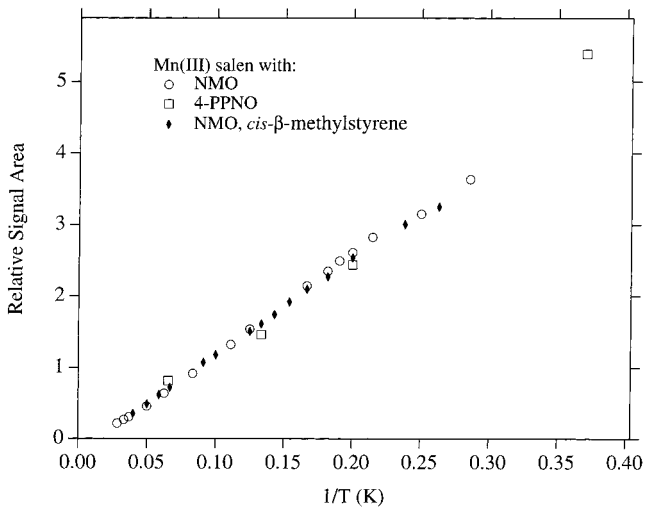

Figure 4. Temperature dependence of the parallel polarization CW-EPR signals of Mn(III) salen with NMO or 4-PPNO. The temperature dependence of Mn(III) salen in CH_2Cl_2 with NMO and *cis*-β-methylstyrene is also shown (solid diamonds). Each point represents the integrated area of the CW-EPR signal at the given temperature. Experimental conditions are the same as Figure 1, except the temperature, which is varied.

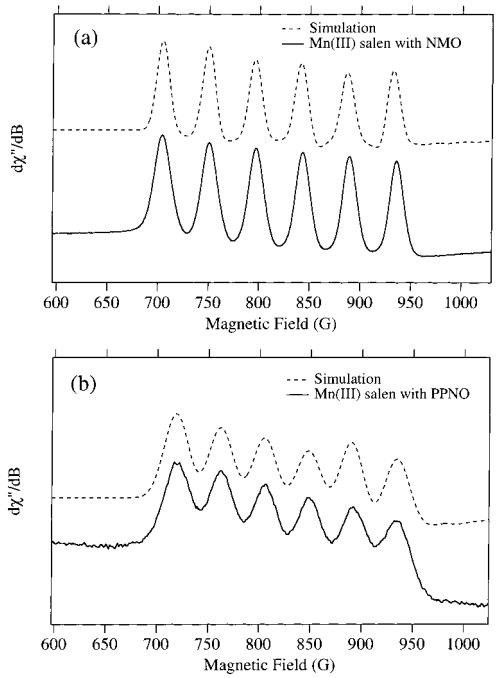

Figure 5. Simulations of the parallel mode EPR of Mn(III) salen in the presence of NMO (A, dotted trace) and in the presence of 4-PPNO (B, dotted trace). The simulations are shown compared to the experimental data (solid traces). Experimental conditions are given in Figure 1. Simulation parameters for the NMO sample are the following: microwave frequency, 9.393 GHz; $D = -2.5$ cm^{-1}; $E = 0.269$ cm^{-1}; $g_\perp = 2.0$; $g_z = 1.98$; $A_\perp = 68$ G; $A_\parallel = 45$ G; line width, 6 G; temperature, 4.4 K; $\theta = 0.1$ to 89.7° in increments of 0.2°; $\phi = 0.1$ to 88.1° in increments of 8°. Simulation parameters for the 4-PPNO sample are the same as in the NMO case except $E = 0.249$ cm^{-1}, $A_\parallel = 42.5$ G, and line width = 12 G.

The temperature dependence of the parallel mode EPR spectrum shows that different hyperfine lines have distinct temperature dependences (Figure 3). This is indicative of the observed transitions arising from either (1) a distribution of Mn(III) centers with different geometries that give rise to different zero-field splitting parameters, (2) different M_s manifolds for a well-defined Mn(III) geometry, (3) dimerization of two Mn(III) ions with either antiferromagnetic or weakly ferromagnetic exchange coupling between the Mn(III) ions with different spin-states populated at different temperatures, or (4) higher nuclearity Mn(III) clusters. There is variation in the overall line shape between prepared samples, possibly due to freezing with

different orientations or molecular distributions when multiple species are present (e.g. dimers or higher nuclearity clusters). The spectra obtained in the presence of *cis*-β-methylstyrene are similar to those obtained in its absence indicating that *cis*-β-methylstyrene does not bind to or alter the magnetic properties of the Mn(III) salen species.

Conversely, in the presence of either NMO or 4-PPNO (Figure 1), the Mn(III) salen complex shows six well-resolved hyperfine lines, indicative of a well-defined molecular geometry about the Mn(III) center with no significant distribution of zero-field splitting parameters. The temperature dependence of the parallel mode EPR signals for Mn(III) salen with 4-PPNO and NMO shows Curie-law behavior (Figure 4), as does the Mn(III) salen/NMO complex in the presence of *cis*-β-methylstyrene. This Curie-law behavior is indicative of an $S = 2$ electron spin system for the d^4 Mn(III) system, with a negative axial zero-field splitting value, D.[18] The EPR spectra of the Mn(III) salen species in the presence of 4-PPNO or NMO arise from transitions between the $M_s = \pm 2$ levels, which are the lowest energy levels when the axial zero-field splitting value is negative. Although the parallel mode EPR spectra for the Mn(III) salen complexes with NMO and 4-PPNO are similar, their hyperfine splittings are slightly different. The Mn(III) salen-NMO complex displays hyperfine lines that are split by approximately 46 G, whereas the Mn(III) salen-4-PPNO complex hyperfine lines are separated by approximately 42 G. The effective g-value at the center of the six lines in each case is also slightly different, 8.16 (NMO) and 8.10 (4-PPNO). These differences, along with the parallel mode EPR signal temperature dependence data, allow for accurate spectral simulations and determination of the parallel hyperfine tensor value ($A_{||}$), g-tensor value ($g_{||}$), and zero-field splitting parameters (D and E). The Mn(III) salen-NMO EPR spectrum is simulated (Figure 5a) with $D = -2.50\ \text{cm}^{-1}$, $E = 0.269\ \text{cm}^{-1}$, $A_\perp = 68$ G, $A_{||} = 45$ G, $g_\perp = 2.0$, and $g_{||} = 1.98$. The Mn(III) salen-4-PPNO EPR spectrum is simulated (Figure 5b) with $D = -2.50\ \text{cm}^{-1}$, $E = 0.249\ \text{cm}^{-1}$, $A_\perp = 68$ G, $A_{||} = 42.5$ G, $g_\perp = 2.0$, and $g_{||} = 1.98$. In an octahedral field, the Mn(III) ^{5}D ground-state term will split into $^5T_{2g}$ and ^5E_g terms. The degeneracy of the ^5E_g ground state will be removed by spin−orbit coupling and Jahn−Teller distortions to give rise to either a $^5A_{1g}$ or $^5B_{1g}$ ground state. Given the simulated zero-field splitting values, $A_{||}$, and $g_{||}$, the ground state term is most likely the $^5B_{1g}$ term with the $d_{x^2-y^2}$ orbital empty, which results in an elongation of the d_{z^2} orbital. Thus, both the NMO and 4-PPNO additive cases are simulated quite well using parameters that are indicative of axially elongated six-coordinate Mn(III) centers.[18] Note that, unlike the parallel turning points, $g_\perp$ and $A_\perp$ are not measurable from the EPR spectra and the EPR simulations are thus not sensitive to these values. From the parallel mode EPR spectra and our simulations, we selected values of $g_\perp$ and $A_\perp$ typical for axially elongated six-coordinate Mn(III) ions.

The perpendicular mode EPR spectra of the Mn(III) salen species with and without additives (Figure 2) demonstrate that the Mn(III) center is also observed with the conventional EPR magnetic field (perpendicular) orientation, at g ≈ 8.1. However, the perpendicular mode spectra do not show hyperfine structure as well-resolved as the parallel mode spectra. Additionally, the perpendicular mode EPR signal amplitudes are much smaller.

Mn(III) Salen Epoxidation Reactions Using NaOCl. The perpendicular and parallel polarization EPR spectra for the expoxidation of *cis*-β-methylstyrene with Mn(III) salen without an additive (Method 1, reaction A) are shown in Figure 6, parts a and b, respectively, over the time course of 0 to 120 min.

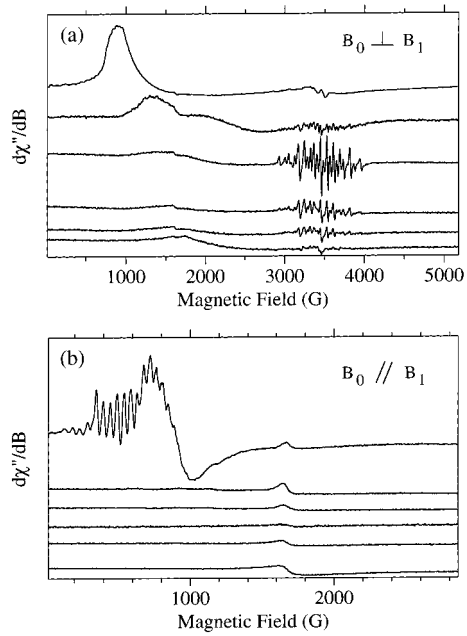

Figure 6. (a) Perpendicular and (b) parallel mode CW-EPR spectra obtained during the reaction time course of Mn(III) salen in CH_2Cl_2 with *cis*-β-methylstyrene before and after the addition of NaOCl (Method 1, reaction A). The traces in parts a and b, from top to bottom, correspond to 0 s (prior to addition of NaOCl) and 3 min 40 s, 20 min, 40 min, 60 min, and 120 min after the addition of NaOCl. Experimental conditions are as in Figure 2 for the perpendicular mode spectra and Figure 1 for the parallel mode spectra. In (a), a Mn(III,IV) dinuclear species EPR signal is apparent near $g = 2$ (≈3450 G) with more than 16 hyperfine lines. At 3 min 40 s, a signal from Mn(IV) is observable near $g \approx 5.1$ (1340 G). The peak around $g \approx 3.9$ (1750 G), apparent after the reaction has run for 120 min, is from another Mn(IV) species.

The Mn(III) salen parallel mode spectrum collected at 2.7 K after the addition of *cis*-β-methylstyrene, but prior to the addition of NaOCl, is shown in the top trace of Figure 6b. After 3 min into the reaction, no Mn(III) parallel mode signal is observable, indicating that virtually all of the Mn(III) species has been oxidized. The peak at ≈1600 G present in each trace of Figure 6b is due to oxygen and is present in almost all parallel mode spectra, as are other background features around 1000 G (seen best in the second and third traces in Figure 6b).[26] The perpendicular mode EPR spectra obtained during the reaction time course are more interesting (Figure 6a). The Mn(III) salen signal is also observable in perpendicular mode at $g \approx 8.1$ prior to the addition of NaOCl (top trace, Figure 6a). The formation of a Mn(IV) species at $g \approx 5.1$ is apparent in the perpendicular mode spectrum collected 3 min after the addition of NaOCl to the Mn(III) salen/styrene mixture (Figure 6a, second trace from top). This Mn(IV) species gives an EPR spectrum similar to a previously reported EPR spectrum for Mn(IV)$(SALADHP)_2$ where the Mn(IV) inner coordination sphere is asymmetric and consists of 2 nitrogen atoms and 4 oxygen atoms.[27a] In addition, an EPR signal from a Mn(III,IV) dinuclear complex grows in at $g = 2$ (≈ 3450 G).[27b] The Mn(III,IV) species signal intensity increases during the reaction course with a corresponding decrease in the initially observed $g \approx 5.1$ Mn(IV) signal intensity. As the reaction nears completion, the Mn(III,IV) species signal intensity decreases, corresponding to a loss of the Mn(III,IV) species. After the disappearance of the Mn(III,IV) EPR signal, the initial Mn(IV) species does not reappear. Instead, a peak grows in at $g \approx 3.9$ (approximately 1750 G).

(26) Smirnov, A. I.; Clarkson, R. B.; Belford, R. L. *EPR Newslett.* **2000**, *11*, 9−11.

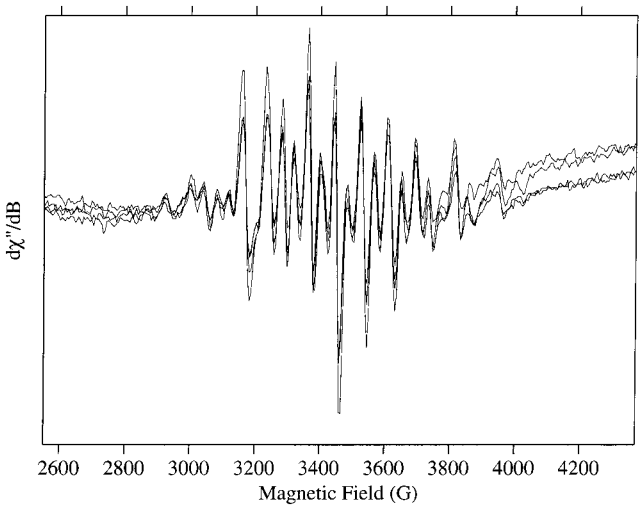

Figure 7. Comparison of the perpendicular mode Mn(III,IV) dinuclear species EPR spectra obtained in four independent trials of the Mn(III) salen reaction with NaOCl 20 min after the addition of NaOCl to the Mn(III) salen (Method 1, reaction A). Notice the similar signal intensities and line shapes. Experimental conditions are the same as for Figure 2.

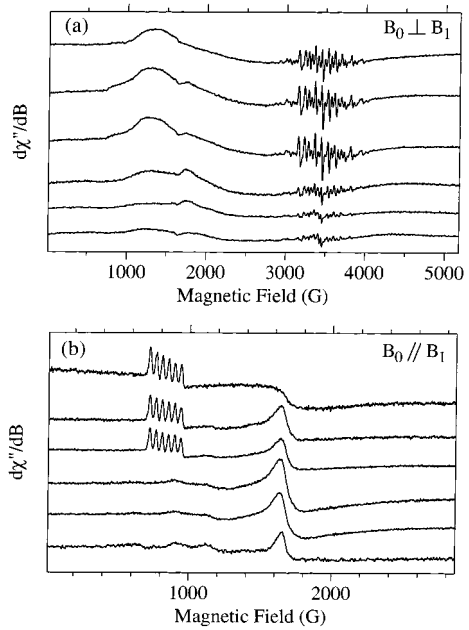

Figure 8. (a) Perpendicular and (b) parallel mode CW-EPR spectra obtained during the reaction time course of Mn(III) salen in CH_2Cl_2 with 4-PPNO and *cis*-β-methylstyrene after the addition of NaOCl (Method 1, reaction B). The traces in parts a and b, from top to bottom, correspond to 10 s, 38 s, 1 min, 5 min, 10 min, and 30 min after the addition of NaOCl. In part a the Mn(III,IV) dinuclear species and the Mn(IV) species signals are apparent as described in Figure 6a. Additionally, the Mn(IV) peak at $g \approx 3.9$ appears much more rapidly after addition of NaOCl (at 38 s compared to 3 min). In part b, the Mn(III) salen/4-PPNO complex is visible as the six-line signal between 800 and 1000 G. The large peak at approximately 1600 G and the three small peaks at 600, 900, and 1100 G are background signals common in parallel mode spectra, most likely due to oxygen. Experimental conditions are as in Figure 2 for the perpendicular mode spectra and Figure 1 for the parallel mode spectra.

This peak is due to a different Mn(IV) form and resembles that observed from Mn(IV)$(HIB)_3$ (HIB = hydroxyisobutyric acid), which has an inner coordination sphere of six oxygen atoms with a trigonal compression along the face defined by three

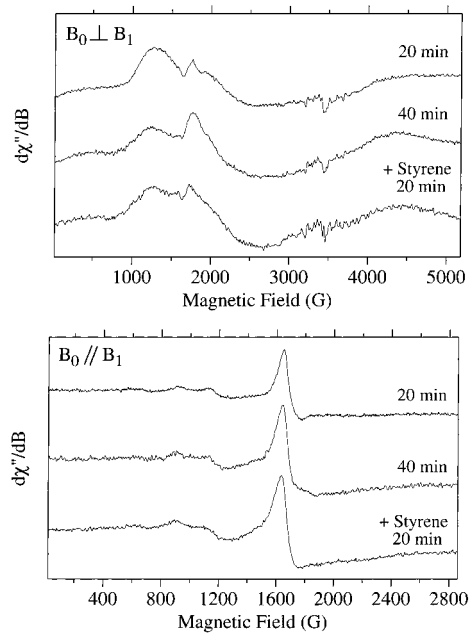

Figure 9. Perpendicular (top graph) and parallel (bottom graph) polarization CW-EPR spectra of a control experiment in which Mn(III) salen in CH_2Cl_2 was reacted with NaOCl without the addition of any styrene to the batch reaction (Method 1, reaction D). No Mn(III,IV) species EPR signal was observed during the control reaction. However, the Mn(IV) peak at 1750 G was present in the control experiment and seemed to increase in amplitude as the reaction proceeded. After 40 min reacting in the absence of styrene, styrene was added. 20 min after styrene addition (bottom trace, top graph) a very small amount of hyperfine structure was observable near $g = 2$; however, the signal never fully resolved, making its assignment to the same Mn(III,IV) species not possible. The parallel polarization spectra (bottom graph) did not show any features above the background during the control reaction.

alkoxide oxygen atoms.[27a] Adam et al.[19b] also recently observed, with ES-MS, an inactive Mn(IV) species ([Mn(IV)(salen)-(Cl)]$^+$OCl$^-$) in a similar epoxidation reaction. Independent trials of this epoxidation reaction show the same EPR spectra over the reaction time course. The Mn(III,IV) species EPR spectrum is identical in each trial as illustrated in Figure 7, which shows an overlay of the Mn(III,IV) EPR spectrum 20 min into the reaction for four independent trials. Prior to observation of the Mn(III,IV) species EPR signal, no epoxide was detected by thin-layer chromatography (TLC); however, in samples for which the Mn(III,IV) species was observed with EPR, epoxide was detected with TLC.

The perpendicular and parallel mode EPR spectra observed during the epoxidation reaction in the presence of 4-PPNO (Method 1, reaction B) are shown in Figure 8, parts a and b, respectively, for the reaction time course from 10 s to 30 min. The epoxidation reaction in the presence of 4-PPNO is completed much more rapidly than the corresponding reaction without 4-PPNO. The EPR spectra for this reaction are similar to the spectra observed for the reaction without 4-PPNO (Figure 6), except that the Mn(III,IV) species appears rapidly and is clearly present in the spectrum taken 10 s after addition of NaOCl in the presence of the additive (Figure 8a, top trace). The Mn(III,IV) species EPR spectrum is similar in the reactions with and without 4-PPNO. The Mn(IV) $g \approx 3.9$ peak appears to grow in (Figure 8a) with the corresponding reduction of the Mn(III,IV) signal, as in the reaction without the 4-PPNO (Figure 6a).

Control experiments were performed with Mn(III) salen

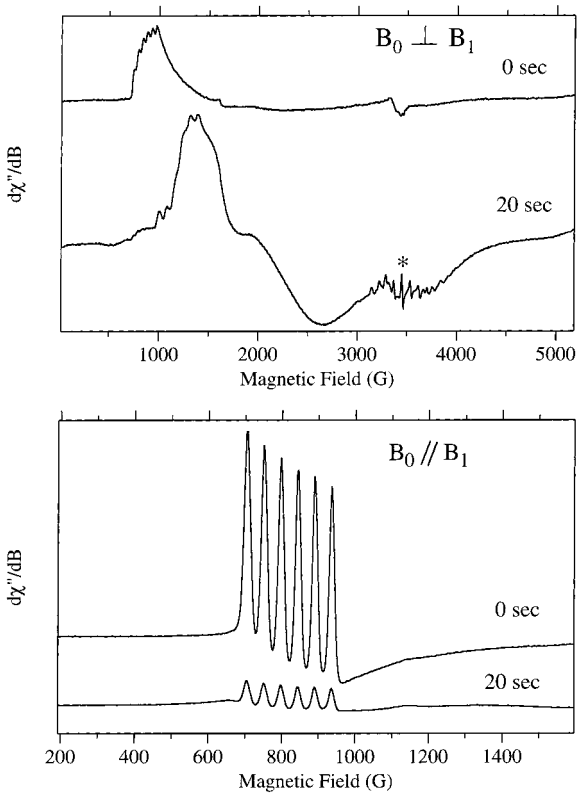

Figure 10. Perpendicular (top graph) and parallel (bottom graph) polarization CW-EPR spectra of Mn(III) salen/NMO and *cis*-β-methylstyrene (Method 1, reaction C). Before addition of *m*-CPBA the Mn(III) salen/NMO signal is observable in both perpendicular and parallel modes (labeled "0 sec"). 20 s after addition of *m*-CPBA, the Mn(III) salen/NMO is almost completely consumed. The perpendicular mode spectra show the formation of a Mn(III,IV) dinuclear cluster species and a Mn(IV) species. The asterisk in the top graph denotes a possible radical species. Experimental conditions are given in Figures 1 and 2 for parallel and perpendicular mode spectra, respectively.

without styrene (Method 1, reaction D). Aliquots for EPR analysis were removed at time points of 20 to 40 min after the addition of NaOCl (Figure 9). The control sample EPR spectra show the disappearance of the Mn(III) salen parallel mode EPR signal immediately after addition of NaOCl (data not shown), and the corresponding appearance of a Mn(IV) EPR signal in the perpendicular mode spectra at $g \approx 3.9$. Additionally, a Mn(IV) species at $g \approx 5.1$ is present in all of the control perpendicular mode EPR spectra (Figure 9a). It is notable that no Mn(III,IV) dinuclear species EPR signal is ever observed in the absence of *cis*-β-methylstyrene, an indication that *cis*-β-methylstyrene is necessary to form the Mn(III,IV) species. NMR and TLC both show the absence of any epoxide formation in this control reaction. The Mn(IV) $g \approx 3.9$ feature that grows in after the completion of the epoxidation reaction with and without 4-PPNO (Figures 6 and 8) is present in all of the control experiment spectra. These results imply that the generation of the $g \approx 3.9$ Mn(IV) species is indicative of inactive Mn salen catalyst, consistent with the inactive Mn(IV) species previously observed by Adam et al.[19b] Interestingly, spectra obtained 20 min after the addition of *cis*-β-methylstyrene to the control reaction mixture that had previously reacted with NaOCl for 40 min show a very slight indication of the formation of a Mn(III,IV) species at $g = 2$ (Figure 9a, bottom trace); however, no epoxide is detected with TLC.

Mn(III) Salen Epoxidation Reactions Using *m*-CPBA. The EPR results for the epoxidation reaction carried out in the presence of NMO using m-CPBA as an oxidant (Method 1, reaction C) are shown in Figure 10. When m-CPBA is used as an oxidant the reaction is completed rapidly (within minutes). The parallel mode EPR results (Figure 10, bottom graph) show the Mn(III) salen/NMO signal taken prior to and 20 s after the addition of m-CPBA. After reacting with the m-CPBA for 20 s, the Mn(III) salen is almost 90% reacted, as evidenced by the decrease in the parallel mode EPR signal. The perpendicular mode EPR spectra (Figure 10, top graph) show a similar reduction in the Mn(III) salen signal (small residual peak at $g \approx 8.1$) and a Mn(IV) signal at $g \approx 5.1$ that has appeared by 20 s after addition of *m*-CPBA. In addition to the Mn(IV) signal at $g \approx 5.1$, a signal is visible at $g = 2$ with at least 11 hyperfine lines, indicative of a ^{55}Mn dimer species. Also at $g = 2$ there appears to be a radical EPR signal (marked by an asterisk). It is possible that this radical is an unwanted byproduct formed due to the oxidizing strength of *m*-CPBA, since a corresponding radical species is not detected in the reaction that proceeds with NaOCl.

The EPR tube reaction (Method 2, Reaction A) time course produced the perpendicular and parallel mode EPR spectra shown in Figure 11, parts a and b, respectively. The EPR tube was successively warmed at a temperature slightly above 175 K and the EPR spectra were recorded after each warming period from 0 to 20 min 15 s. The top traces in Figures 11a and 11b show the perpendicular and parallel mode EPR spectra, respectively, obtained prior to allowing the top layer of *m*-CPBA to react with the bottom Mn(III) salen/NMO/styrene layer. The subsequent traces of Figure 11a and 11b (second from top to bottom) correspond to the EPR spectra obtained after warming for 30 s, 1 min 15 s, 2 min 45 s, 4 min 45 s, 7 min 45 s, 10 min 15 s, 15 min 15 s, and 20 min 15 s, respectively. The Mn(III) salen/NMO signal present in both the perpendicular and parallel mode spectra near $g \approx 8.1$ can be seen to disappear as the tube is warmed. Corresponding to the disappearance of the Mn(III) signal, a Mn(IV) signal appears near $g \approx 5.1$ in the perpendicular mode spectra. The Mn(IV) species appears to form initially at a higher field than observed in the final reaction trace. The vertical line in Figure 11a is drawn through the maximum of the Mn(IV) peak in the final reaction product (bottom two traces); however, at the earlier reaction times, the Mn(IV) peak is significantly shifted upfield (by at least 100 G). This indicates that the Mn(IV) species present at early times in the reaction is in a different environment from the Mn(IV) species present at the completion of the reaction.

The parallel mode EPR spectra (Figure 11b) for the reaction carried out in an EPR tube (Method 2, reaction A) show successive disappearance of the Mn(III) salen/NMO complex signal. Interestingly, a new peak appears downfield from the lowest field peak of the six-line signal (most visible in the third and fourth traces from the bottom of Figure 11b). This peak actually corresponds to the low-field peak of a new six-line EPR signal, as confirmed by the following freeze-quench experiments.

The freeze-quench experiments (Method 3, reaction A) clearly show this new parallel mode EPR signal at 50 and 64 ms into the reaction of the Mn(III) salen/NMO/stryene mixture with *m*-CPBA (Figure 12a). A comparison of the 50 and 64 ms mixing time parallel mode signals with the signal taken prior to mixing (Figure 12a, top trace) shows the presence of new signals at very low field (20 G) and to slightly lower field of the six-line Mn(III) hyperfine signal (at approximately 655 G) in the 50 and 64 ms traces. The Mn(III) salen EPR signal amplitude has decreased by approximately half after the reaction

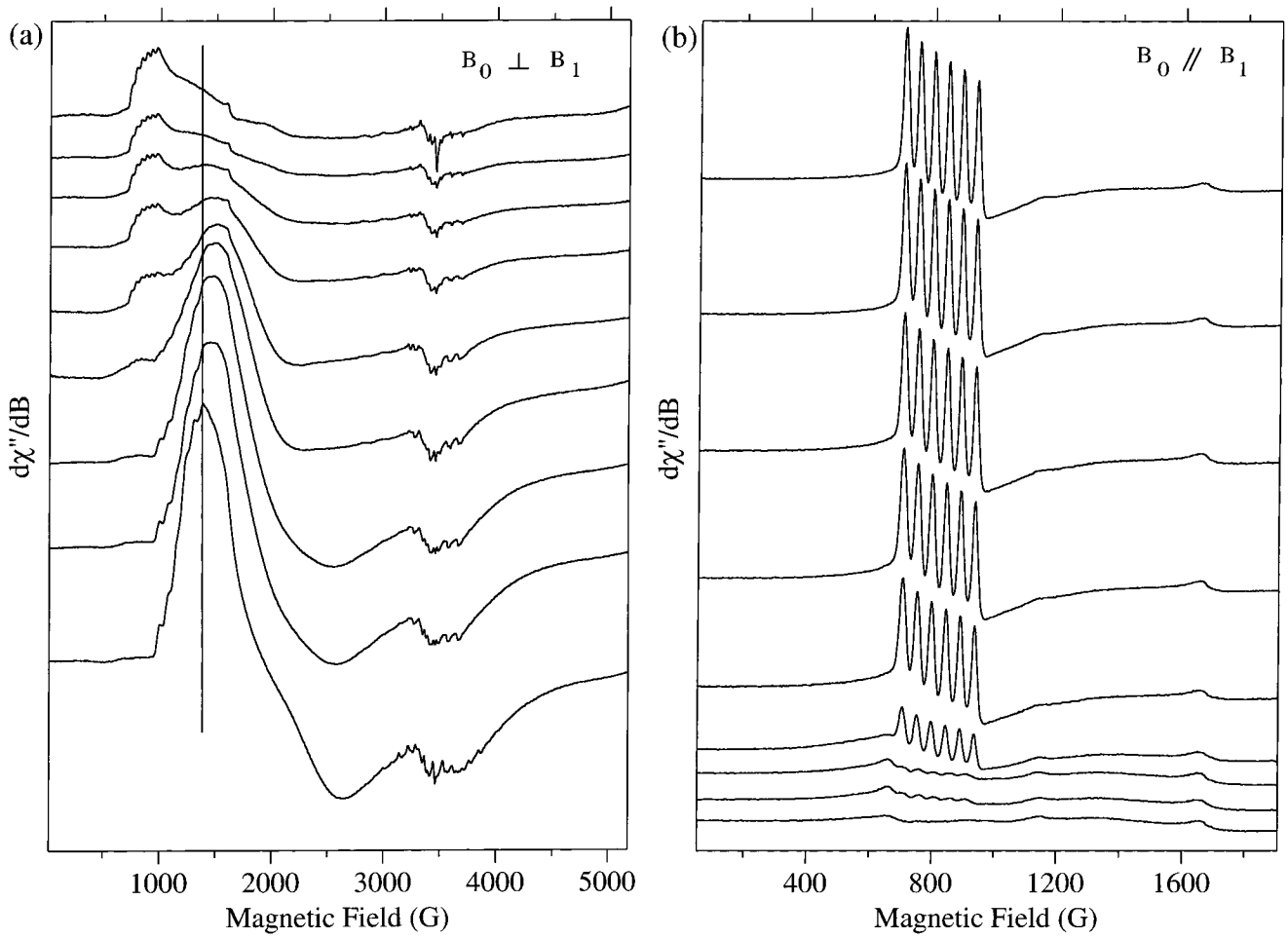

Figure 11. (a) Progression of the perpendicular mode spectra obtained via the EPR tube reaction (Method 2, reaction A) after successive warming slightly above 175 K. The top trace is the unreacted sample with the *m*-CPBA layer on top of the Mn(III) salen/NMO/styrene layer. The subsequent traces are obtained after warming the EPR tube slightly above 175 K for a total of (second from top to bottom) 30 s, 1 min 15 s, 2 min 45 s, 4 min 45 s, 7 min 45 s, 10 min 15 s, 15 min 15 s, and 20 min 15 s, respectively. Experimental conditions are the same as for Figure 2. (b) Parallel mode CW-EPR spectra corresponding to the perpendicular mode spectra given in part a. The six-line signal centered around 800 G is from the Mn(III) salen/NMO complex. Experimental conditions are as given in Figure 1.

has proceeded for 50 ms. The low-field peak at approximately 20 G could be from either an integer or half-integer spin species; since it is a low-field signal, the orientation of the applied oscillating magnetic field either parallel or perpendicular to the static magnetic field has little effect on the transition probability for observation of this signal. Thus, the same signal is observed in the perpendicular mode EPR spectra (Figure 12b; 50 and 64 ms traces and to a lesser extent the 500 ms trace). It is possible that this signal arises from a short-lived Mn(V)═O species in the $S = 1$ spin state. However, because the signal has no hyperfine structure and is present in both perpendicular and parallel mode spectra, it is not possible to simulate accurately at this time.

Close inspection of the regions between the Mn(III) salen hyperfine lines in the 50 and 64 ms parallel mode EPR spectra (Figure 12a) shows small shoulder peaks which correspond to ^{55}Mn hyperfine structure. Notice that the peak at 655 G is much larger at 64 ms than it is at 50 ms. Correspondingly, the Mn(III) salen hyperfine peaks are larger at 50 ms than at 64 ms. This implies that the Mn(III) salen/NMO species is transformed into a new species that gives rise to the shifted six-line hyperfine structure. This new EPR signal, absent in the perpendicular mode, could be from a Mn(III) ion in a coordination environment different from the initial Mn(III) salen species, or possibly from an $S = 1$ or 2 Mn(V) species.

The perpendicular mode EPR traces corresponding to the freeze-quench 50, 64, and 500 ms reaction times (Figure 12b) show the presence of an EPR signal near $g = 2$ corresponding to a radical species. This species appears slightly larger after 500 ms than at 50 ms. This radical signal was also observed in the EPR spectrum obtained from the batch reaction, Method 1, reaction C (Figure 10), 20 s into the reaction. The freeze-quench results also show that the line shape of the derivative-shaped peak at 2300 G appears to change as the reaction progresses. This could be due to a change in the coordination environment of a Mn(IV) species. All of the freeze-quench perpendicular mode traces show greater than six ^{55}Mn hyperfine lines near $g = 2$. This implies some formation of a ^{55}Mn dimer species very early in the reaction course.

Conclusions

The perpendicular mode EPR spectra for Mn(III) salen with and without NMO have been previously attributed to a Mn(III) salen species[28] based on comparison of the effective *g*-values

(27) (a) Pecoraro, V. L. Structurally Diverse Manganse Coordination Complexes: From Voodoo to Oxygenic Photosynthesis. In *Manganese Redox Enzymes*; Pecoraro, V. L., Ed.; VCH Publishers: New York, 1992; pp 199−204. (b) Larson, E. L.; Pecoraro, V. L. Introduction to Manganese Enzymes. In *Manganese Redox Enzymes*; Pecoraro, V. L., Ed.; VCH Publishers: New York, 1992; pp 1−28.

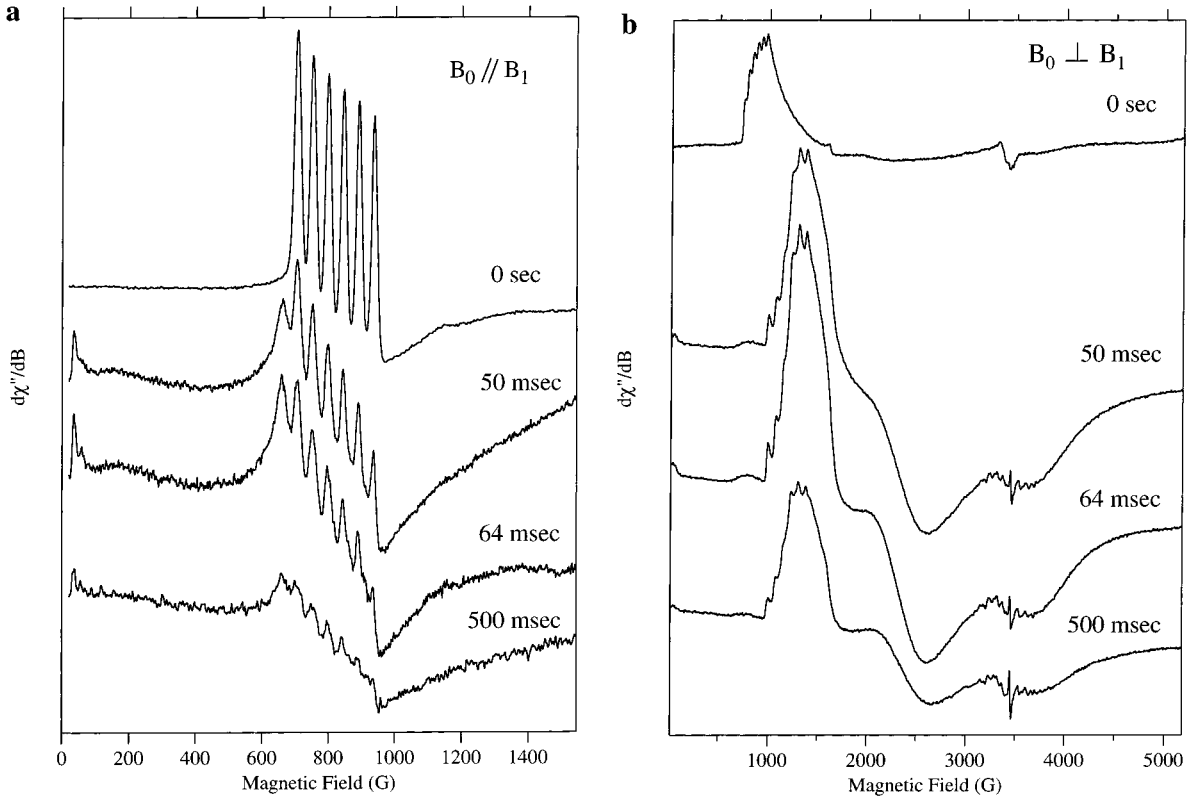

Figure 12. (a) Parallel mode CW-EPR spectra obtained before mixing (labeled "0 sec") and 50, 64, and 500 ms after mixing the Mn(III) salen/NMO/*cis*-β-methylstyrene mixture with the *m*-CPBA mixture (Method 3, reaction A). Experimental conditions are as given in Figure 1. (b) Perpendicular mode CW-EPR spectra corresponding to the parallel mode spectra given in part a. Experimental conditions are as given in Figure 2.

and hyperfine spacings with those of the manganese(III) acetylacetonate species (55 G)[29] and Mn(III) trapped in TiO_2 (53 G).[30] Using parallel polarization CW-EPR which allows direct observation of the Mn(III) species,[18] we confirm that the perpendicular mode $g \approx 8$ signal in the Mn(III)/NMO complex is indeed due to a Mn(III) species. The parallel polarization EPR signal of the Mn(III) salen complex in the absence of an additive is ^{55}Mn hyperfine rich. Although we have presented several possibilities for the origin of this complex spectrum, we favor an explanation that two or more Mn(III) centers are coupled in the absence of NMO or 4-PPNO. If there was a distribution of Mn(III) centers with different geometries, one would expect a broad, sinusoidal parallel mode spectrum without resolved ^{55}Mn hyperfine structure due to the distribution of molecular geometries. Also, we have not been able to simulate the EPR spectrum with a Mn(III) ion in a well-defined geometry with zero-field splitting values that allow for transitions between various M_s levels and that match the observed temperature dependence of the EPR transitions.

In contrast to previous reports,[5] the parallel mode spectra of Mn(III) salen in the presence of NMO and 4-PPNO reflect that these ligands alter the ligand field around the initially five-coordinate Mn(III) salen metal center by binding to Mn(III) *before* the formation of any reaction species. The negative axial zero-field splitting value ($D = -2.5$ cm^{-1}) and the hyperfine and **g**-tensor values obtained from the EPR spectral simulations

Scheme 1

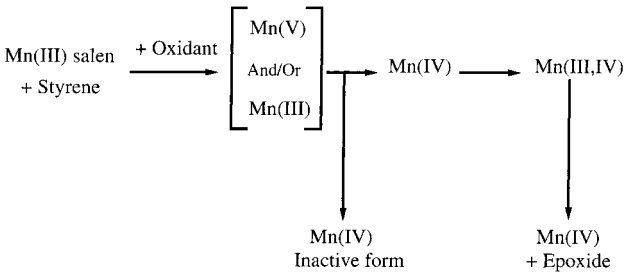

in both additive cases are indicative of an axially elongated six-coordinate Mn(III) complex. The parallel mode EPR data suggest that the additives may improve reaction yields and reaction rates by dissociating any multiple nuclearity Mn(III) centers and returning them to well-defined monomeric Mn(III) states available for the epoxidation reaction. Another possibility is that the elongation of the d_{z^2} orbital, triggered by the additive binding, makes it more accessible to the olefin. Both of these factors most likely contribute to the enhanced success of reactions with additives.

Control experiments in which the reaction was run without styrene did not show formation of the Mn(III,IV) species. Additionally, reactions run with styrene under conditions with limited NaOCl showed very little epoxide and Mn(III,IV) dinuclear cluster formation. Thus the observation of a Mn(III,IV) species during the epoxidation reaction is indicative of a Mn(III,IV) dinuclear cluster intermediate.

A complication to determining the Mn(III) salen-catalyzed epoxidation reaction mechanism is the possibility that many factors may influence the reaction pathway. These include the Mn(III) salen ligands,[2,4,32] the type of alkene,[31] the additive (donor ligand),[5,13−16] the reaction solvent, the oxidizing agent,

(28) Bryliakov, K. P.; Babushkin, D. E.; Talsi, E. P. *Mendeleev Commun.* **1999**, 29−32.
(29) Dexheimer, S. L.; Gohdes, J. W.; Chan, M. K.; Hagen, K. S.; Armstrong, W. H.; Klein, M. P. *J. Am. Chem. Soc.* **1989**, *111*, 8923−8925.
(30) Gerritsen, H. J.; Sabisky, E. S. *Phys. Rev.* **1963**, *132*, 1507−1512.
(31) Fu, H.; Look, G. C.; Zhang, W.; Jacobsen, E. N.; Wong, C.-H. *J. Org. Chem.* **1991**, *56*, 6497−6500.
(32) Sasaki, H.; Irie, R.; Hamada, T.; Suzuki, K.; Katsuki, T. *Tetrahedron* **1994**, *50*, 11827−11838.

and the temperature.[1] However, as shown in this study, the advantage of the dual-mode EPR technique is that it not only provides a very sensitive probe to changes in the ligand environment of the Mn(III) center, it also enables one to spectroscopically follow the reaction progress as a function of reaction time, allowing the simultaneous observation of the Mn(III) salen catalyst and the formation of Mn intermediates, radical intermediates, and Mn byproducts. Based on our results, we suggest that the epoxidation reaction mechanism corresponding to our experimental conditions includes the Mn species shown in Scheme 1. The EPR data do not provide enough information to assign all of the ligands to all of the observed Mn species accurately. However, Scheme 1 is a reasonable guide to the oxidation states of Mn observed during the reaction time course.

Coupled with the freeze-quench experiments which show promise for detection of either a Mn(V) intermediate and/or a Mn(III) species involved in the early ligand coordination, the dual-mode EPR technique will provide significant insight into the Mn(III) salen-catalyzed epoxidation reactions of various substrates under a wide variety of experimental conditions. Further experiments are focusing on continued elucidation of the reaction course at early reaction times using freeze-quench trapping techniques along with dual-mode EPR spectroscopy.

JA0027463